J. Magn. Soc. Jpn., **41**, 29-33 (2017)

<Paper>

Development of MO imaging plate for MO color imaging

Y. Nagakubo, Y. Baba, Q. Liu, G. Lou, and T. Ishibashi

Department of Materials Science and Technology, Nagaoka University of Technology, *1603-1 Kamitomioka, Nagaoka, Niigata 940-2188, Japan*

We propose a magneto-optical (MO) color imaging technique that enables magnetic field distributions to be quantitatively observed in real-time. Values of magnetic fields are displayed as colors. MO imaging plates have been developed using highly bismuth-substituted neodymium iron garnet films, for use in MO color imaging. The films were prepared by the metal-organic decomposition method. The MO imaging plates were characterized using the MO figure of merit for MO imaging plates, which is defined in this study. The magnetic fields were expressed by colors, using light-emitting diodes (LEDs) as light sources. The colors varied from blue to yellow, from green to yellow, and from blue to red, for sources corresponding to a white LED, combined green and yellow LEDs, and combined blue and yellow LEDs, respectively. The MO color imaging of spherical magnets is demonstrated.

Key words: magneto-optical imaging, bismuth substituted neodymium iron garnet, magneto-optical effect, metal organic decomposition, magneto-optical imaging plate, magneto-optical figure of merit

1. Introduction

The MO imaging technique utilizes the magneto-optical (MO) effect of bismuth-substituted iron garnet. The technique was developed separately by Japanese and Russian groups in 1990, to visualize stray magnetic fields from superconducting materials[1), 2)]. MO imaging allows magnetic field distributions to be observed in real-time, by placing MO imaging plates at locations to be measured[1)-9)]. MO imaging can achieve a high spatial resolution of ~0.3 μm[8), 10)], and a high speed response with frequencies up to ~1 GHz[11)]. Computational calculations for each pixel in a measured MO image are conventionally required to obtain a quantitative image of the magnetic field[4)-6)]. To realize quantitative MO imaging, we propose a MO color imaging technique that enables quantitative magnetic field distributions to be observed in real-time and values of magnetic fields are displayed as colors. We expect the resolution of the displayed magnetic field to be improved by using color instead of monochrome. Specifically, the resolution of the magnetic field in color could potentially be the cube of that in monochrome. For example, in the case of an 8-bit camera, magnetic field values could be expressed with $2^{8\times3}$ = 16777216 colors, compared with 2^8 = 256 in monochrome.

MO imaging plates are expected to have properties suitable for MO color imaging. Large MO imaging plates are required to observe magnetic field distributions with the naked eye. Bi-substituted rare-earth iron garnets ($R_{3-x}Bi_xFe_5O_{12}$: Bi:RIGs) have traditionally been used as materials for MO imaging plates. These are usually prepared by the liquid phase epitaxy method. However, it is difficult to achieve a high Bi substitution, and the size of films is limited by that of the single crystal substrate such as $Gd_3Ga_5O_{12}$ (GGG), which is typically smaller than 4 inches in diameter[12)-14)]. To overcome these problems, we prepared highly Bi-substituted neodymium iron garnet ($Nd_{3-x}Bi_xFe_{5-y}Ga_yO_{12}$) films, by metal-organic decomposition (MOD) on glass and GGG substrates[15)]. This allows larger MO imaging plates to be prepared.

In this paper, we discuss the MO figure of merit for MO imaging plates prepared using $Nd_{0.5}Bi_{2.5}Fe_5O_{12}$ (Bi2.5:NIG) or $NdBi_2Fe_5O_{12}$ (Bi2:NIG), and we report the use of the MO imaging plates in quantitative MO color imaging.

2. Experimental

Bi2.5:NIG and Bi2:NIG thin films were prepared by the MOD method on glass and GGG substrates[16)-18)]. Bi2.5:NIG and Bi2:NIG were selected as the MO films for the MO imaging plate. This was because their MO figures of merit were sufficiently high, and their spectral profiles were suitable for MO color imaging. MOD solutions were produced by Kojundo Chemical Laboratory Co., Ltd. The glass substrates used in this study were Eagle XG, Corning. $Nd_2BiFe_4GaO_{12}$ (Bi1:NIGG) thin films with a thickness of 90 nm were prepared as a buffer layer on the glass substrates.

To prepare Bi2.5:NIG, Bi2:NIG and Bi1:NIG thin films, each MOD solution was spin-coated at 3000 rpm on the substrate for 60 s. The resulting film was dried at 100 ºC for 10 min, and then pre-annealed at 450 ºC for 10 min. This process of spin-coating to pre-annealing was repeated five times. The resulting film was then crystallized in a furnace at 600–700 ºC for 3 h in air. The process was repeated several times, to increase the film thickness. Ag alloy (APC, Furuya Metal Co., Ltd.) films of approximately 100 nm in thickness were deposited on the garnet layers as reflection layers, using a coater (SC-704, Sanyu Electron Co., Ltd.).

The MO and optical properties of the MO imaging plates were measured, to evaluate the MO figure of merit. Faraday and Kerr rotation spectra were measured using a MO spectrometer (Neoark Co., Ltd.). The spectrometer consisted of a halogen lamp, polarizer,

monochromator, electromagnet, and polarization angle detector. The spectrometer setup was based on the balanced detection method. Transmission spectra were measured using a spectrometer (V-570, JASCO Corp.).

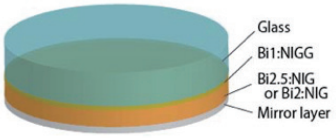

Fig. 1 Structure of the MO imaging plate prepared on a glass substrate.

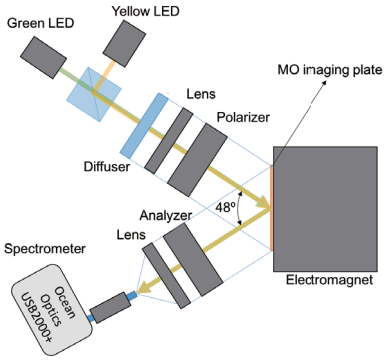

Fig. 2 Schematic illustration of the experimental setup.

The experimental setup shown in Fig. 2 was used for MO color imaging. The light source was a white LED, or combined green and yellow LEDs, or combined blue and yellow LEDs. The applied magnetic field range of the electromagnet (AZ1-0, Toei Scientific Industrial Co., Ltd.) was set from −3 kOe to +3 kOe. MO images were collected using a CMOS camera, and spectra were measured using a spectrometer (USB2000+, OceanOptics). The angle of the polarizer and analyzer were set at 0 and 84°, respectively. This combination of angles was found to result in the largest color change, upon application of the magnetic field. The relationship between the color and magnetic field was then calibrated, to create the color scale.

3. Results and Discussion

3. 1 Figures of merit for the MO imaging plates

Faraday rotation spectra of Bi2.5:NIG films prepared on glass substrates at annealing temperatures of 600–700 °C are shown in Fig. 3. Kerr rotation spectra of the same samples containing mirror layers are shown in Fig. 4. The thickness of the Bi2.5:NIG film was approximately 450 nm. Periodic structures are clearly observed in both figures, which arose due to interference of the light in the garnet layers. This indicated that the samples had optically smooth surfaces. The Faraday rotation spectra exhibited maxima at around 530 nm in wavelength, and were consistent with previous reports[15), 16)]. The Kerr rotation spectra exhibited maxima at 590–620 nm in wavelength, and their Kerr rotation angles were larger than the Faraday rotation angles at the same wavelength. However, the peaks in the Kerr rotation spectra at 530 nm were smaller than the Faraday rotation angles at the same wavelength, which was attributed to optical losses. The figure of merit of a magneto-optical material is usually defined as[19)-21)],

$$Q = 2\,|\theta_F| / \alpha = 2\,|\theta_F|\, t / ln\,(1/T) \quad \text{(deg.)}, \ (1)$$

where θ_F (deg./μm) is the Faraday rotation angle, $\alpha = t / ln(1/T)$ is the absorption coefficient, T is the transmittance, and t is the thickness of the MO film. However, equation (1) is unsuitable for determining the figure of merit of the current MO imaging plates. An effective rotation angle of the polarization plane should decrease with optical losses. This is due to optical absorption of the MO layer, and reflection at the substrate surface and at the interface between the substrate and MO film. Therefore, we define the figure of merit for the current MO imaging plates using the Kerr rotation angle θ_K, according to,

$$Q' = |\theta_K|\, t / ln(1/T) = |\theta_K'| / ln(1/T)\ \text{(deg.)}, \quad (2)$$

where θ_K (deg./μm) and θ_K' (deg.) is the Kerr rotation angle, T is the transmittance, and t is the thickness of the MO film.

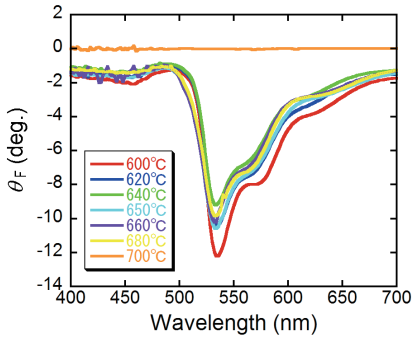

Fig. 3 Faraday rotation angles of MO imaging plates containing Bi2.5:NIG films annealed at 600–700 °C.

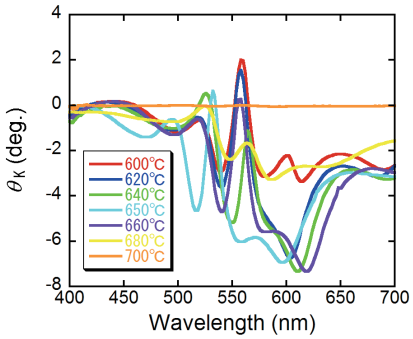

Fig. 4 Kerr rotation angles of MO imaging plates containing Bi2.5:NIG films annealed at 600–700 °C.

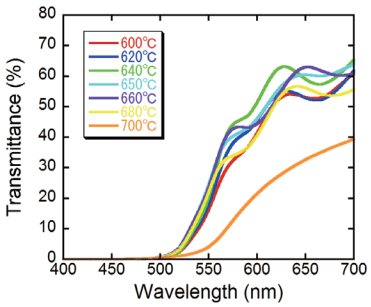

Fig. 5 Transmission spectra of MO imaging plates containing Bi2.5:NIG films annealed at 600–700 °C.

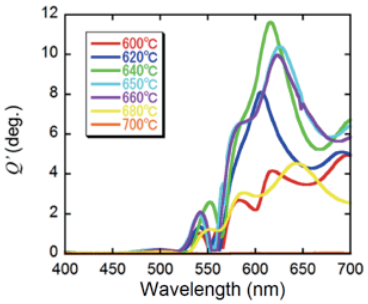

Fig. 6 MO figures of merit for MO imaging plates containing Bi2.5:NIG films crystallized at 600–700 °C.

Figures of merit Q' of the MO imaging plates as defined by equation (2) are shown in Fig. 6. Samples crystallized at 620–660 °C exhibited higher MO figures of merit at wavelengths of 580–650 nm. The highest figure of merit was obtained at a wavelength of 615 nm for the sample crystallized at 640 °C.

In MO imaging, in addition to the figure of merit of the MO imaging plates, the light source spectrum must also be considered. Spectra of the light sources used in the current study are shown in Fig. 7. A sharp peak at 450 nm and a broad peak at 525–625 nm were observed in the spectrum of the white LED, as shown in Fig. 7(a). Peaks at 530 and 600 nm were observed in the spectrum of the combined green and yellow LEDs, as shown in Fig. 7(b). Peaks at 470 and 600 nm were observed in the spectrum of the combined blue and yellow LEDs, as shown in Fig. 7(c). For MO imaging with the white LED, the Q' should be multiplied by the spectrum of the white LED, as shown in Fig. 8. Fig. 8 shows that under these conditions, the MO imaging plates could operate in the wavelength range of 570–650 nm, i.e. yellow-red.

3.2 MO color imaging

To develop MO color imaging to quantitatively determine the magnetic field, values of the magnetic field were calibrated for color. MO images and intensity spectra of a pole of the electromagnet were measured with a CMOS camera and spectrometer, respectively, using the experimental set up shown in Fig. 2. A MO imaging plate with a Bi2.5:NIG garnet film crystallized at 640 °C was used in this experiment, and the white LED was used as the light source. Fig. 9 shows intensity spectra of the reflected light, and MO images of the pole of the electromagnet, measured under applied magnetic fields of −1, 0, and +1 kOe. The colors were blue for −1 kOe, violet for 0 kOe, and yellow for +1 kOe. The intensity of the reflected light at a wavelength of 550–650 nm increased as the applied magnetic field increased in the positive direction. This corresponded to negative Kerr rotation. The profiles of the intensity spectra in Fig. 9 were consistent with the spectrum in Fig. 8. The intensity at 550 nm slightly increased as the applied magnetic field increased in the negative direction. A peak at 450 nm is observed in the spectrum in Fig. 9. This was derived from the peak of the white LED. The intensity of this peak was independent of the applied magnetic field, as the Q' was almost zero at the wavelength of 450 nm.

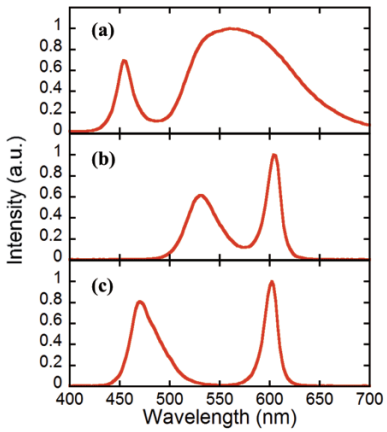

Fig. 7 Spectra of the (a) white LED, (b) combined green and yellow LEDs, and (c) combined blue and yellow LEDs, which were used as light sources.

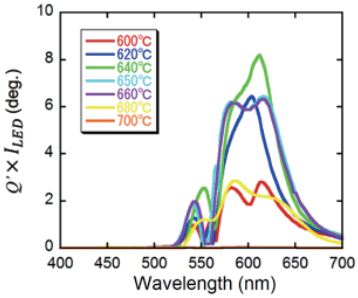

Fig. 8 Figures of merit of the MO imaging plates multiplied by the spectrum of the white LED.

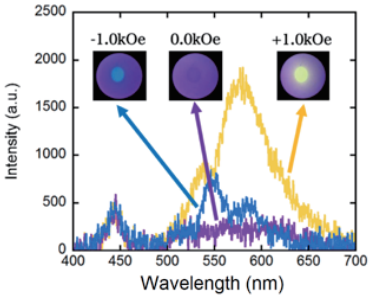

Fig. 9 Intensity spectra of the reflected light, and MO images of the pole of the electromagnet, measured under applied magnetic fields of −1, 0, and +1 kOe.

The result when using the combined green and yellow LEDs as the light source is shown in Fig. 10. Fig. 10(a) shows the Kerr rotation spectrum of a MO imaging plate containing the Bi2:NIG film used in this experiment. The Kerr rotation angles were +4 and −7 degrees at wavelengths of 530 and 595 nm, respectively. The Kerr rotation angle at 530 nm was larger than that of Bi2.5:NIG. This was because the transmittance at 530 nm of the MO imaging plate containing the Bi2:NIG film was higher. Peaks are observed at 530 and 600 nm in the intensity spectra in Fig. 10(b). These peaks increased asymmetrically with increasing applied magnetic field, as shown in Fig. 10(b). This resulted in the color becoming green at −1.0 kOe, dark green at 0.0 kOe, and yellow at +1.0 kOe. The asymmetric behavior of the intensities of these two peaks can be explained by the Kerr rotation spectrum in Fig. 10(a). The Kerr spectrum contained peaks at 530, 540, and 600 nm which are involved in this phenomenon. The sign of the Kerr rotation at 530 nm was opposite to those at 540 and 600 nm, and the angle of the analyzer was rotated −6° from the cross-polarized position. Therefore, the intensity at 530 nm decreased from −2 kOe to +0.5 kOe, and then increased. In contrast, the intensity at 600 nm increased from −0.5 kOe with applied magnetic field.

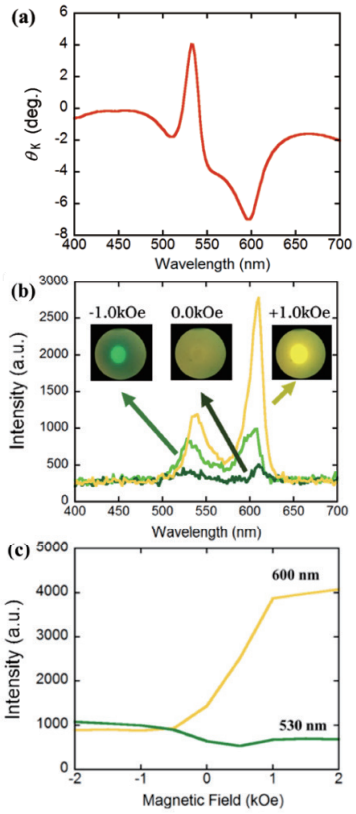

Fig. 10 (a) Kerr spectrum of the Bi2:NIG film on the glass substrate, (b) intensity spectra of the reflected light, and MO images of the pole of an electromagnet measured, at −1, 0, and +1 kOe, and (c) dependence of light intensity on applied magnetic field, at wavelengths of 530 and 600 nm.

Fig. 11 shows the MO images of the pole of an electromagnet measured using the white LED, combined green and yellow LEDs, and combined blue and yellow LEDs, as light sources. The colors changed from blue to yellow, from green to yellow, and, from blue to red, respectively, with changing magnetic field. This constituted color scales corresponding to the magnetic field. Quantitative color values were obtained as RGB values, which were deduced from the measured spectra. Values for the xy colorimetric system were then obtained from the RGB values. The three curves corresponding to the data in Fig. 11 are plotted in the chromaticity diagram (CIE1931) in Fig. 12. The magnetic field values were quantitatively evaluated with colors.

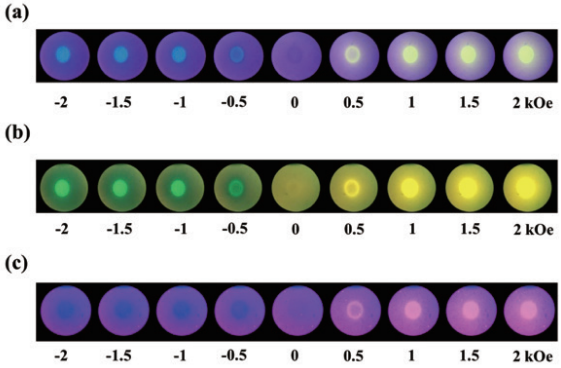

Fig. 11 MO images of the pole of an electromagnet, in which the light source was (a) a white LED, (b) combined green and yellow LEDs, and (c) combined blue and yellow LEDs.

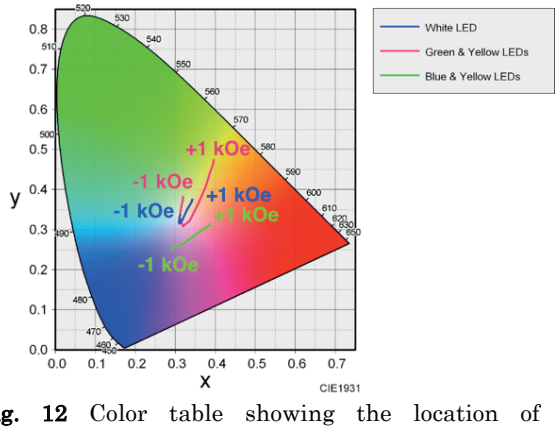

Fig. 12 Color table showing the location of experimentally-obtained data using the white LED, green and yellow LEDs, and blue and yellow LEDs as light sources.

Quantitative MO color imaging using the white LED is demonstrated in Fig. 13. Connected spherical neodymium magnets were measured as a sample, which is shown in Fig. 13(a). A color scale prepared using the procedure described above is shown together with an MO image in Fig. 13(b). The MO image shows the quantitative distribution of the magnetic fields directly above the magnets. South (S) and north (N) magnetic poles are indicated by blue and yellow, respectively, and

zero points are indicated by violet. The magnetic fields could also be expressed in RGB values.

Kerr rotation spectra of various garnet films with different film compositions and substrate types are shown in Fig. 14. The spectral profiles strongly depended on the film composition and substrate material. However, the spectral profiles could potentially be modeled by optical simulations, if the optical constants including the permittivity tensors are known[22].

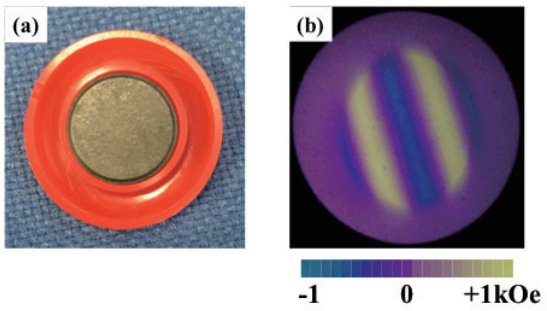

Fig. 13 (a) Digital photograph of spherical magnets, and (b) corresponding MO color image.

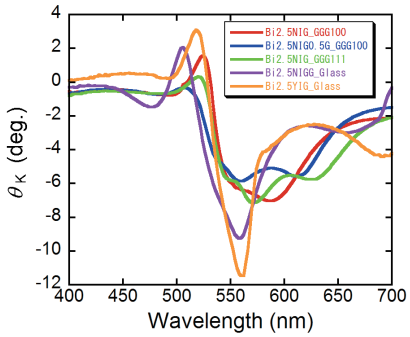

Fig. 14 Kerr rotation spectra of various garnet films with different film compositions and substrate types.

4. Conclusions

We have developed a MO imaging plate containing Bi2:NIG and Bi2.5:NIG films for MO color imaging. The MO figure of merit for the MO imaging plates defined in this study accurately represents their MO properties with respect to MO imaging. The MO imaging plates using Bi2.5:NIG exhibited a high MO figure of merit in the 570–650 nm wavelength range. The color varied from blue to yellow, as the magnetic field changed from −2 to +2 kOe, when using a white LED. The color changed from green to yellow, or from blue to red, when combined green and yellow LEDs and combined blue and yellow LEDs were used as light sources, respectively. A color scale indicating values of the magnetic field was obtained, along with a MO color image of a ferrite magnet. These collectively displayed the intensity and pattern of the magnetic field in color.

Acknowledgement

The authors thank Dr. Yongfu Cai for technical assistance with experiments.

References

1) S. Gotoh, N. Koshizuka, M. Yoshida, M. Murakami, and S. Tanaka: *Jpn. J. Appl. Phys.*, **29,** L1083 (1990).
2) M. V. Indenbom, N. N. Kolesnikov, M. P. Kulakov, I. G. Naumenko, V. I. Nikitenko, A. A. Polyanskii, N. F. Vershinin, and V. K. Vlasko-Vlasov: *Physica C*, **166,** 486 (1990).
3) T. H. Johansen, and D. V. Shantsev: *Magneto-Optical Imaging, NATO Science Series II Mathematics, Physics, and Chemistry*, (Kluwer Academic, Dordrecht 2004) pp.1-10.
4) Ch. Joose, A. Forkl, R. Wrthmann, H.-U. Hbermeier, B. Leibold, and H. Kronmüller: *Physica C*, **266**, 235 (1996).
5) Ch. Joose, J. Albrecht, H. Kuhn, S. Leonhardt, and H. Kronmüller: *Rep. Prog. Phys.*, **65,** 651 (2002).
6) T. Ishibashi, Z. Kuang, S. Yufune, T. Kawata, M. Oda, T. Tani, Y. Iimura, K. Sato, Y. Konishi, K. Akahane, X. Zhao, and T. Hasegawa: *J. Appl. Phys.*, **100**, 093903 (2006).
7) L. A. Dorosinskii, M. V. Indenbom, V. I. Nikitenko, Yu. A. Ossip'yan, A. A. Polyanskii, and V. K. Vlasko-Vlasov: *Physica C*, **203**, 149 (1992).
8) T. Ishibashi, G. Lou, A. Meguro, T. Hashinaka, M. Sasaki, and T. Nishi: *Sensors and Materials*, **27**, 965 (2015).
9) W. C. Patterson, N. Garraud, E. E. Shorman, and D. P. Arnold: *Rev. Sci. Instrum.*, **86,** 094704 (2015).
10) M. Takahashi, K. Kawasaki, H. Ohba, T. Ikenaga, H. Ota, T. Orikasa, N. Adachi, K. Ishiyama, and K. I. Arai: *J. Appl. Phys.*, **107**, 09E711 (2010).
11) N. Adachi, D. Uematsu, T. Ota, M. Takahashi, K. Ishiyama, K. Kawasaki, H. Ota, K. Arai, S. Fujisawa, S. Okubo, and H. Ohta: *IEEE Trans. Magn.*, **46**, 1986 (2010).
12) K. Iida, N. Kawamae, S. Hoshi, T. Machi, T. Kono, J. Yoshioka-Kato, N. Chikumoto, N. Koshizuka, N. Adachi, and T. Okuda: *Jpn. J. Appl. Phys.*, **44**, 1734 (2005).
13) H. Lee, T. Kim, S. Kim, Y. Yoon, S. Kim, A. Babajanyan, T. Ishibashi, B. Friedman, and K. Lee: *J. Magn. Magn. Mater.*, **322**, 2722 (2010).
14) T. Kono, T. Machi, N. Chikumoto, K. Nakao, N. Koshizuka, N. Adachi, and T. Okuda: *J. Magn. Soc. Jpn.*, **30**, 600 (2006).
15) T. Yoshida, K. Oishi, T. Nishi, and T. Ishibashi: *EPJ Web Conf.*, **75**, 05009 (2014).
16) G. Lou, T. Yoshida, and T. Ishibashi: *J. Appl. Phys.*, **117**, 17A749 (2015).
17) T. Ishibashi, T. Yoshida, T. Kobayashi, S. Ikehara, and T. Nishi: *J. Appl. Phys.*, **113**, 17A926 (2013).
18) T. Kosaka, M. Naganuma, M. Aoyagi, T. Kobayasi, S. Niratisairak, T. Nomura, and T. Ishibashi: *J. Magn. Soc. Jpn.*, **35**, 194 (2011).
19) P. Hansen, K. Witter, and W. Tolksdorf: *Phys. Rev. B*, **27**, 6608 (1983).
20) A. M. Grishin, S. I. Khartsev, and S. Bonetti: *Appl. Phys. Lett.*, **88**, 242504 (2006).
21) S. Kang, S. Yin, V. Adyam, Q. Li, and Y. Zhu: *IEEE Trans. Magn.*, **43**, 3656 (2007).
22) E. Jesenska, T. Yoshida, K. Shinozaki, T. Ishibashi, L. Beran, M. Zahradnik, R. Antos, M. Kučera, and M. Veis: *Optical Materials Express*, **6**, 1986 (2016).

Received Oct. 11, 2016; Accepted Jan. 10, 2017